Prairie View A&M University AUV Robotics: Transitioning from the Panther to the PV Inspire

Viareakoudom Long, Renel Allen, Patierre Thorpe, Uzair Nadeem, Qamiyon Marshall, Shelby Williams, Jovondi Williams

***Abstract*— The Prairie View A&M Autonomous Underwater Vehicle (PV AUV) Robotics Team is an undergraduate team comprised of mechanical, electrical, and computer engineering students under the advisement of respective professors from within the Roy G. Perry College of Engineering. Innovations in autonomous subsea robots have been extremely valuable. To the oil and gas industry these robots perform several underwater functionalities such as, but not limited to, mapping underwater terrain for potential oil reservoirs or monitoring and quickly fixing piping leaks. Through the exploitation and reimaging of existing technologies and methods utilized to manufacture current autonomous underwater vehicles (AUVs), the team designed, engineered, and programmed the *PV Inspire* to compete in the 2018 International RoboSub Competition.**

Entities that employ AUVs to do subsea work desire a robot that is intelligent and equipped to respond to a variety of underwater challenges quickly without any external assistance. Aiming to satisfy competition goals and provide solutions to industry matters, *the PV Inspire* is fashioned to exceed its predecessor *the Panther* in overall functionality, capable of interpreting and following visual cues, manipulating the environment, maintaining control under harsh underwater conditions, and executing desired tasks efficiently. The standard eight thruster arrangement paired with an adjustable rod-clamp design ensures a high level of maneuverability and increases the vehicle's overall modularity. A forward-facing camera allows the AUV to scope and follow the pool floor while a servo-operated, also to navigate the vehicle through its surroundings. The vehicle's navigational system, computational boards, and main power source are sealed within a large cylindrical hull, creating a simplistic, yet intricate and lightweight design.

I. Introduction

Established since 2011, PV AUV is a yearly senior design project structured to challenge a collaborative team of engineers of various disciplines to design and build a fully autonomous underwater vehicle, capable of competing in the AUVSI RoboSub Competition. This year students were originally tasked with modifying, and enhancing the autonomy of the Prairie View's AUV, *PV Inspire*. While the original design of the vehicle proved to be, in theory, structurally sound, the overall deterioration of the vehicle's frame, electrical connections, and unresolved water leakage inspired the PV AUV team to push the boundary and design a completely new sub. Hence, the *PV Inspire* was engineered not only to surpass its predecessor in the technical aspect, but to serve as a turning point for the engineering program at Prairie View, inspiring students to go beyond self-imposed limits and aspire to produce products of excellence.

II. Design Strategy

The *PV Inspire* is designed to satisfy four main project objectives: functionality, convenience, safety, and economic consideration. Restricted to primarily in-house fabrication, a limited budget, and a yearly time constraint, the team focused on creating a simple and effective, yet cost-efficient sub. A successful design that incorporates a high degree of modularity and maneuverability, target-tracking capabilities, sonar sensing, and a fully integrated navigational system hypothetically will allow the AUV to meet the basic navigational goals and leave room for future teams to develop the vehicle for additional task items.

In retrospect, previous teams designed a hull to fit a rigid frame and subsequently manipulated the weight and buoyancy according to the addition and placement of external housings. The open-frame design, for example, has a thin cross sectional frame for easy movement in the forward and backward directions. The selected material, Aluminum 6061, meets the demanding strength-to-weight ratio, possesses excellent resistance to corrosion, and is overall considered "good" [1] for underwater vehicle structures. In comparison to earlier variations of the AUV, the frame added a new level of modularity, allowing the thruster mounts to move freely along the horizontal slots. However, the rigid structure configuration, which was designed to fit the hull in its entirety while remaining within the AUVSI maximum size constraints, limited the versatility for other, potential components and left little to no room for any major adjustments along the frame.

Focusing primarily on increasing modularity and reliability without sacrificing capability, this year's team opted to move most of the electronic and software components inside a single hull and design a frame capable of accommodating different shapes and thruster arrangements. The final design of the *PV Inspire*, shown in Fig. 1, emphasizes simplicity and functionality and easily accessible components allowing for the adjustment of current parts and the retrofitting of any additional parts.

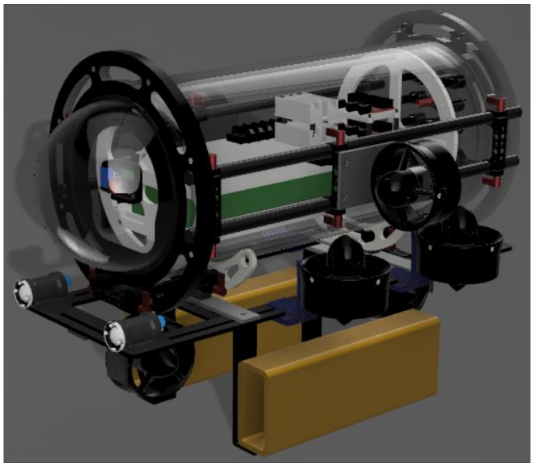

Fig. 1 Autodesk Fusion CAD rendering of the finalized *PV Inspire*

III. Vehicle Design

Initially, the design process was generated and outlined for the schedule, problem identification, project planning, and literature review phases. The team encountered a few technical problems with the literature review and was forced to reformat and clarify the content to demonstrate a solid understanding of AUV components and concepts. However, using Microsoft Projects, the team collaboratively established an estimated timeline and Gantt Chart to meet the anticipated milestones and deliverables, as a well-planned and detailed schedule is key. Additional components were added to the vehicle that was used from the previous 2017 competition such as two l

A. Preliminary Design

By dissecting and grasping the failures and successes of previous design concepts applied to *the Panther*, the team acknowledged common mistakes and incorporated effective techniques and ideas into the current design. The preliminary design of the *Inspire* began with a functional decomposition flow chart that specified the main function the AUV needed to accomplish and sub-functions that explicitly define how the team would enable the vehicle to deliver. Given the difficulties experienced by previous teams in navigation and sensory tasks, the main function consisted of the AUV completing three specified competition tasks: finding the casino, entering the casino (passing through a validation gate), and following a path marker. Enabling the vehicle to move to a specified destination and integrating the electronic components served as the two major sub-functions which shaped the ideas that populated the concept generation chart. Ideas were collectively evaluated and either denoted as a “GO” or a “NO-GO” based on general efficiency, effectiveness, and reliability. From there, ideas denoted as “GO” were discussed at length based on a more detailed set of criteria, considering additional factors such as how much time and funding the team would have to incorporate the concept, manufacturability, longevity, and whether the concept would keep the vehicle lightweight.

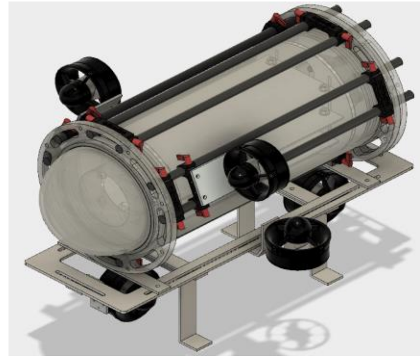

Fig. 2 Autodesk Fusion CAD rendering of the original *PV Inspire*

The modular design displayed in Fig.2 demonstrates the initial compilation of the resulting “GO” concepts' and ideas from the decision-matrix selection process. This original design was implemented as the redesign of *The Panther* of 2017 that implemented sliding clamps and it's respective rails and a support frame that inherited the same level of modularity but on different surface. The previous year model did not implement any additional lighting to aid the camera systems, and needed tremendous amount of weights added to counteract the buoyancy. As shown in Fig 1, those notable drawbacks have been corrected with built in coated steel beam weights permanently attached to the leg support and underwater front beam lights.

Table 1: The Overview of the *PV Inspire*

Specification	**Dimension (units)**
Length	21.5 (inches)
Width	15.0 (inches)
Height	17.3 (inches)
Weight *	35.2 (Pounds)
Max Depth (Tested)	12 (feet)
Thrusters	8 x Blue Robotics T100
Camera(s)	USB camera
Inertial Navigational System	Inertial Measurement Unit (IMU)
Operating Frameworks	Arduino Mega, Intel Celeron

**The listed weight in the table doesn't include any ballasts or additional weights needed to obtain .5% bouyancy*

B. Mechanical Systems

Detailed process and design analysis equations and simulations were applied and conducted on all the AUV’s major components. The gathered results further determined the reliability as well as the robustness of the vehicle and gave deeper insight to hidden failure points. Autodesk Fusion 360, ANSYS, and Siemens NX were all utilized to run analyses on various parts of the *Inspire*. Much of the structure has not changed from the previous year design beyond the additional components to help aid the machines navigation system.

1) Cylindrical Hull

A cylindrical, acrylic hull, which serves as the main housing unit for all the electrical components (including the battery), is the only physical element being reused from *the Panther* [2]. As a transparent material, it allows to quickly diagnose and identify problems even while sealed and submerged underwater, but consequently weaker than other materials such as aluminum and polycarbonate. A thorough hydrostatic analysis was simulated in Autodesk Fusion to ensure structure failure due to increased water pressure would not cause the hull to fail.

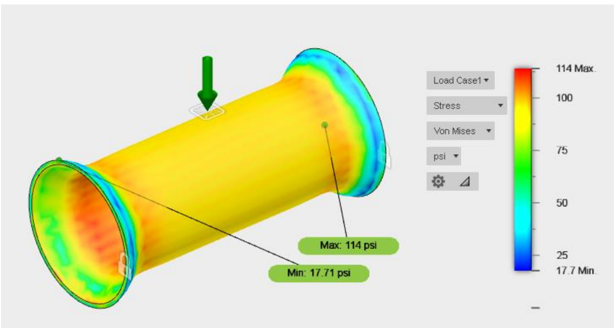

Fig. 3 Stress Analysis for the Hull

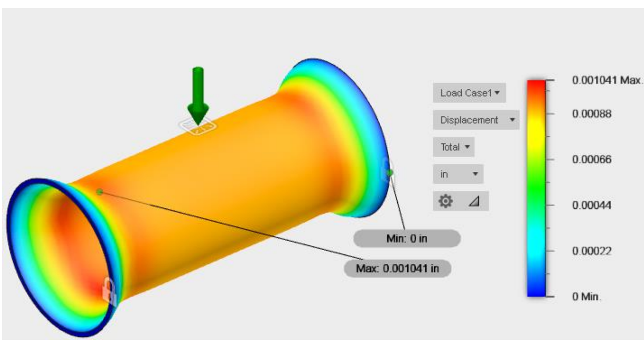

Figure 4. Displacement Analysis for Hull

At a competition depth of 16 feet, the pressure induced on the tube would be estimated to be 6.94 psi (pounds per square inch) as displayed in Fig. 4. Compared to the acrylic yield strength of 7092 psi, hull failure due increasing water pressure was determined to be ineffective. A deflection analysis was also conducted, resulting in a theoretical displacement of no more than .001 inches, which was determined to be insignificant in affecting the inner electronics as well as any detriment to the seals from the endcaps.

2) Hull Endcaps

The hull endcaps are a fundamental yet critical part of the hull sub-assembly, used to create a barrier between the aquatic competition environment and the electrical components housed within the hull's interior. Acrylic endcaps were fabricated to seal the acrylic hull and hold the attached mounting rods which would serve as a surrounding frame. The custom-made aluminum endcaps used in the previous years performed adequately in sealing the electronic components. However due to time constraints and difficulty in processing aluminum, it was determined by using acrylic and not requiring specialized skill set and the simplicity and remanufacturing the endcaps in the acrylic material in case a defect or an upgrade in the design was needed, it would serve to more practical end goal. The team was given the opportunity to remake the endcaps and properly select O-rings using the compression and stretch recommendations, where the material was easier to manipulate as far as its specific dimensions are concerned based on the following inner diameter and cross-sectional diameter equations [3].

$$ID = G_d(1 - S_{rec}) \qquad (1)$$

where,

- ID is the inner diameter of the O-ring
- S_{rec} is the bore diameter tolerance
- G_d is the groove diameter

$$CS \;\; max = \left[\frac{(B_d - B_{tol}) - (G_d + G_{tol})}{2}\right]\left(\frac{1}{1 - C_{max}}\right) - CS_{tol} \qquad (2)$$

$$CS_{min} = \left[\frac{(B_d + B_{tol}) - (G_d - G_{tol})}{2}\right]\left(\frac{1}{1 - C_{max}}\right) + CS_{tol} \qquad (3)$$

where,

- CS_{max} is the maximum cross-sectional diameter of the O-ring,
- CS_{min} is the maximum cross-sectional diameter of the O-ring
- B_d is the bore diameter
- B_{tol} is the bore diameter tolerance
- G_d is the groove diameter
- G_{tol} is the groove diameter tolerance
- C_{max} is the maximum compression
- CS_{tol} is the cross-sectional tolerance

The stretch of the O-ring references how snuggly the seal fits into the groove, based on its circumferential stretch. A great seal will generally have a preferred stretch within 2% of its inner diameter value. Additionally, the O-ring will compress radially once it has settled in the gland. To meet the recommended maximum compression of 40%, the cross-sectional diameter of the O-ring must be greater than the overall effective depth of the groove.

The calculations for equations (1-3) were conducted in Engineering Equation Solver (EES) to theoretically determine the inner diameter and cross section of the O-ring needed to achieve an ideal seal compression against water. As a result, the following tables were generated, displaying all possible sizes, both standard and custom-made, that would provide the best seal for the acrylic endcaps. The tables displayed in Fig. 5-7, depict these results. The blue highlight indicates the base standard against which all other variations were compared. Purple indicates O-rings that failed the specified stretch and compression criteria. The yellow highlight represents results that were plausible but concerning. The manila shade represents results that were still plausible but more likely to succeed due to certain exceptions. Finally, the green specifies results that were highly plausible and likely to properly seal the hull. To save time, all of the O-ring sizes that produced green results were purchased and manually tested for the best fit.

AS-568 Chart Comparison | ISO O-ring 3601 Chart Comparison | "Other O-ring sizes" -Apple Rubber Comparison

2..8	ID [in]	CS [in]	G_d [in]	S_{rec}	C [%]	GW [in]	OD
Run 1	7.526	0.1911	7.68	0.02	16.27	0.2867	8.062
Run 2	7.25	0.125	7.64	0.05105	-44	0.1875	7.89
Run 3	7.5	0.125	7.79	0.03723	16	0.1875	8.04
Run 4	7.25	0.1875	7.663	0.0539	10.13	0.2813	8.038
Run 5	7.5	0.1875	7.69	0.02471	17.33	0.2813	8.065
Run 6	7.75	0.1875	7.69	-0.007802	17.33	0.2813	8.065
Run 7	7.25	0.25	7.6	0.04605	20	0.375	8.1

Fig. 5 Side view of the Rear Acrylic Endcap

AS-568 Chart Comparison | **ISO O-ring 3601 Chart Comparison** | "Other O-ring sizes" -Apple Rubber Comparison

2..8	ID [in]	CS [in]	G_d [in]	S_{rec}	C [%]	GW [in]	OD
Run 1	7.526	0.1911	7.68	0.02	16.27	0.2867	8.062
Run 2	7.234	0.139	7.62	0.05068	-36.69	0.2085	7.898
Run 3	7.484	0.139	7.768	0.03658	16.55	0.2085	8.046
Run 4	7.734	0.139	7.768	0.004403	16.55	0.2085	8.046
Run 5	7.225	0.2098	7.6	0.04933	4.691	0.3148	8.02
Run 6	7.475	0.2098	7.65	0.02288	16.59	0.3147	8.07
Run 7	7.725	0.2098	7.72	-0.0006477	33.27	0.3147	8.14
Run 8	7.225	0.2751	7.55	0.04305	18.21	0.4127	8.1

Fig. 6 Side view of the Rear Acrylic Endcap

AS-568 Chart Comparison | ISO O-ring 3601 Chart Comparison | **"Other O-ring sizes" -Apple Rubber Comparison**

2..23	ID [in]	CS [in]	G_d [in]	S_{rec}	C [%]	GW [in]	OD
Run 1	7.526	0.1911	7.68	0.02	16.27	0.2867	8.062
Run 2	7.244	0.158	7.7	0.05922	5.063	0.237	8.016
Run 3	7.224	0.315	7.68	0.05938	49.21	0.4725	8.31
Run 4	7.283	0.177	7.68	0.05169	9.605	0.2655	8.034
Run 5	7.283	0.197	7.648	0.04772	10.66	0.2955	8.042
Run 6	7.283	0.209	7.644	0.04723	14.83	0.3135	8.062
Run 7	7.283	0.236	7.6	0.04171	15.25	0.354	8.072
Run 8	7.402	0.158	7.73	0.04243	14.56	0.237	8.046
Run 9	7.402	0.236	7.605	0.02669	16.31	0.354	8.077
Run 10	7.48	0.158	7.735	0.03297	16.14	0.237	8.051
Run 11	7.48	0.197	7.67	0.02477	16.24	0.2955	8.064
Run 12	7.48	0.209	7.65	0.02222	16.27	0.3135	8.068
Run 13	7.48	0.236	7.605	0.01644	16.31	0.354	8.077
Run 14	7.559	0.158	7.74	0.02339	17.72	0.237	8.056
Run 15	7.581	0.215	7.65	0.00902	18.6	0.3225	8.08
Run 16	7.61	0.158	7.738	0.01654	17.09	0.237	8.054
Run 17	7.618	0.197	7.69	0.009363	21.32	0.2955	8.084
Run 18	7.638	0.118	7.78	0.01825	6.78	0.177	8.016
Run 19	7.638	0.224	7.64	0.0002618	19.64	0.336	8.088
Run 20	7.677	0.118	7.805	0.0164	17.37	0.177	8.041
Run 21	7.677	0.158	7.75	0.009419	20.89	0.237	8.066
Run 22	7.677	0.236	7.61	-0.008804	17.37	0.354	8.082
Run 23	7.734	0.139	7.77	0.004633	17.27	0.2085	8.048

Fig. 7 Side view of the Rear Acrylic Endcap

A stress analysis was conducted to determine probable failure under 60lbf (pound force) of reactionary force – the result of an extreme weight scenario of the summed AUV weights and components needed to counteract excessive buoyancy. The forces applied to the analysis were originally specified to be the reaction forces from the stress caused by the weight of the AUV, while lifted, with the minimum force that would be required to carry the AUV into water. Both the stress and deflection were minimal and most likely would not cause the geometries to fail, as the results were far beneath the maximum yield strength. The results of the stress and displacement are displayed in Fig. 8 and Fig. 9 respectively.

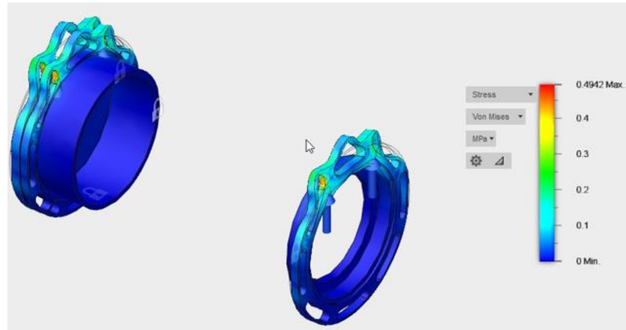

Fig. 8 Stress Analysis of the Front and Back Endcaps

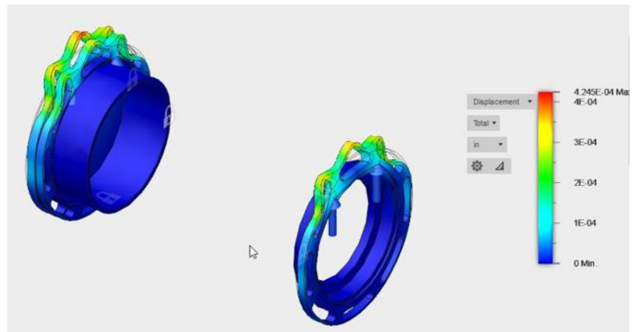

Fig. 9. Displacement Analysis of the Front and Back Endcaps

The acrylic dome, which is acrylic cemented to the front endcap, houses the camera enabling the AUV to have a comprehensive and transparent viewing window. This will allow *the Inspire* to visually interpret the surrounding environment and adjust itself accordingly.

Apart from vision sensory, the dome also serves the purpose of ensuring that vehicle maintains a laminar shape. In Fig. 10, a streamline velocity analysis was conducted through ANSYS to simulate the moving velocity of the AUV through a fluid, or relatively speaking a body of water. Based on the results, the overall geometry of the vehicle does not alter the laminar flow of the vehicle, making it easier for the AUV to maneuver.

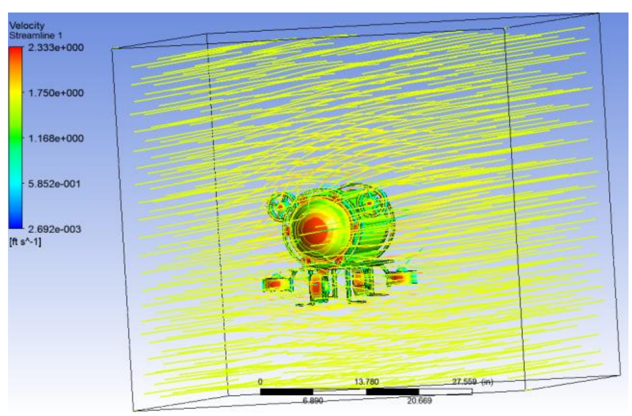

Fig. 10 ANSYS rendering of a Streamline Velocity Analysis (Front View)

3) Thrusters

The Blue Robotics T100 thrusters supply the necessary force to propel the vehicle and allow it to navigate in a desired direction (forward, backward, left, right, up, down). The design of *the PV Inspire* allows each of the eight thrusters to be moved to relatively any position along its respective axis (Fig. 11).

Fig. 11 Example of Thruster Modularity Along Past Platform Base

A hydrostatic pressure contour was conducted to determine the best positioning for the thrusters. The side-thruster configuration displayed in Fig. 12, allows for the best equal distribution of the pressure along the front of the vehicle, rather than in one area. Although the positioning of the side-thrusters appears to perform best at a higher altitude, keeping them aligned with the center of pressure will always yield favorable results.

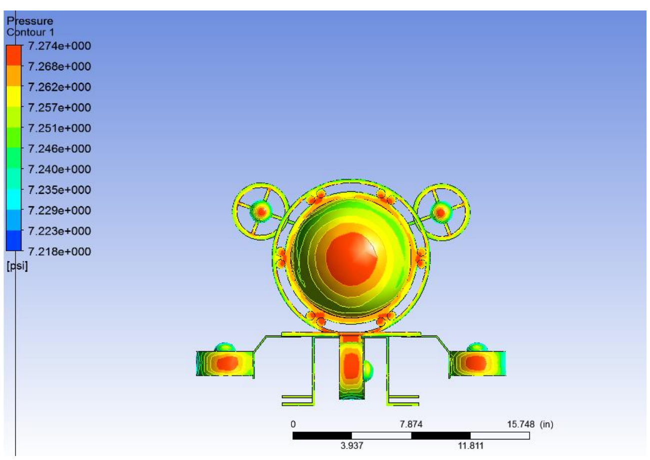

Fig. 12 ANSYS rendering of a Pressure Contour Analysis (Front View)

4) Electronics Rack System

In retrospect, gaining access to electronics within the hull has always been inefficient and ineffective. Generally, once the primary housing unit was removed from the frame, one of the aluminum endcaps served as a foot platform, while the other cap was pried from the opposite end. However, the acrylic material is significantly weaker in comparison to the aluminum, and cannot withstand the same tensile stresses.

Delrin racks were used with fixed position in contrast to the original intent of the racks – to allow adjustment of the levels and spacing. horizontally slot into the end chassis on each side. Instead, a rack was pre-designed to accommodate different configurations and add other mounting holes for components if necessary. threaded rods also screw horizontally through the pre-determined holes to hold the full assembly together. The length of the rack was also expanded to occupy more of the hull space and accommodate more components if necessary. Each part of the electronics rack system was also fabricated using a Model 10000 Epilog Zing Laser as shown in Fig. 13.

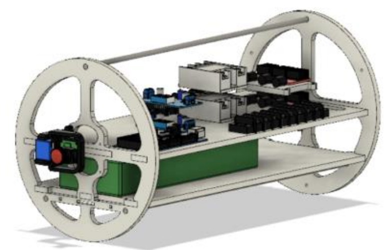

Fig. 13 rendering of a Delrin bases Electronics Rack

5) Frame Rods

The aluminum camera rods appended to the sides of the hull will serve as retrofittable frame for mounting the thrusters, adding dead weight, and other various components deemed necessary upon testing, presently and in the future. Each 15mm (diameter) black aluminum alloy rod is a compilation of one 16-inch and one 4-inch rod, threaded together to achieve a total length of 20-inches. Each rod is positioned around the hull, using the pre-defined slots around the endcaps for alignment. The rod clamps aid in this endeavor, securing the rods in place to prevent sliding and also making the end caps tightly shut.

A stress analysis for the Aluminum 6061 hollow rods was conducted with the attached rod clamps to determine loaded vertical stress and to simulate the stress of the mounted components, such as the thrusters and any additional components that may need to be mounted. The loaded force was tested at 25lbf, which includes the weight force of the thrusters, propulsion, and possible added weights to counteract buoyancy.

The stress was determined to be under 10 kpsi, which is within the range of 3000-8000 psi based on Fig. 14, with the stress concentrated in the center of the rod length based. Even the maximum stressed incurred stayed below the maximum yield of 40kpsi, and caused minimal deflection, as displayed in Fig. 15, with a maximum displacement of .041 inches.

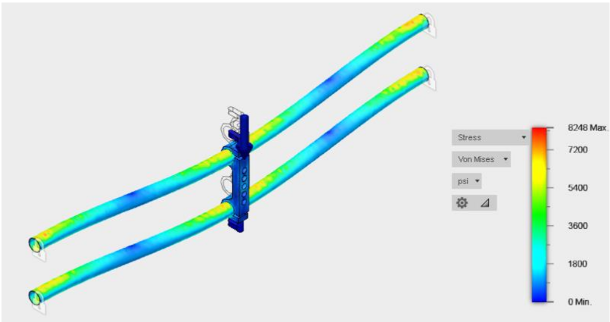

Fig. 14 Von Misses Stress Analysis of Camera Rods with Rod Clamp

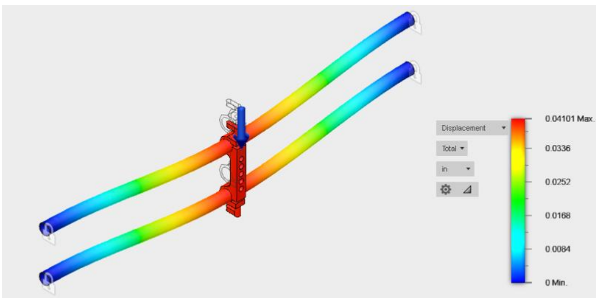

Fig. 15 Displacement Analysis of Camera Rods with Rod Clamp

6) Aluminum Platform Assembly

A computer numerical control (CNC) machine was used to manufacture an aluminum 6061 plate into a mounting platform. The frame from previous years served as a protective barrier around the hull as well as a base for additional components and dead weight to be mounted. With the removal of the rigid frame, added components could only be attached to the aluminum rods surrounding the hull. The original functionality of the platform was to serve as a foundation for the four ground thrusters, two up and down and two side to side.

Fusion 360 was used to find the total buoyant force and the center of buoyancy (CB). As shown in Fig. 16, the assembly is "joined" as a solid piece with uniform density.

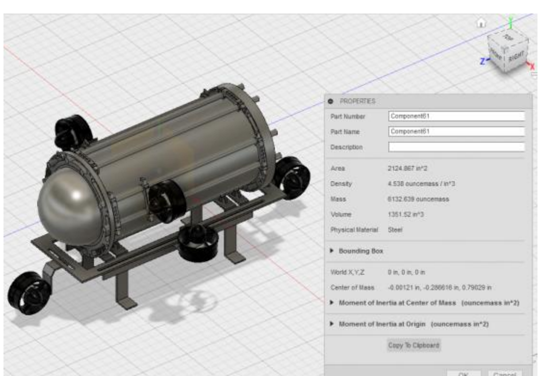

Fig. 16 Autodesk Fusion Rendering of Center of Buoyancy Calculations

For this new piece based off the old design since the primary structure has not changed, the center of mass (CM) function was now able to find the CB of the original piece.

The "Properties" function was then used to show the total volume and CB:

CB (with respect to the origin): {-0.00121 in, -0.286616 in, 0.79029 in}

Volume: 1351.52 in^3

Given the total volume (V) and estimated specific volume of sea water (w), buoyancy (B) can be determined using the relationship [4]:

$$B = Vw \qquad (4)$$

where,

B is the buoyant force,
V is the volume of the displaced fluid, and
w is the specific weight of the fluid (sea water in this case).

Given,

$V = 1351.52\ in^3$

$w = 64\ \frac{lbs}{ft^3}$,

The buoyant force (4) was computed to be 50.56lbs.

The total mass and CM were also calculated using Fusion 360. After the correct individual masses and positions were set, the total mass was found to be roughly 30.4lbs. The "Center of Mass" function was then used, as shown in Fig. 17, and found, directly below the center of buoyancy, indicated by a blue circle (CM) and then a white circle respectively (CB).

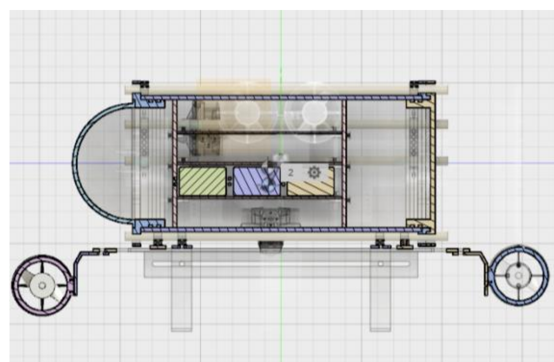

Fig. 17 Autodesk Fusion Rendering of CM and CB Coordinate Results

Additionally, based on the values shown in Table 2, while both the 'x' and 'z' values are roughly the same, the CM is nearly one inch lower than the CB. A visual representation of the results is also incorporated and displayed in Fig. 17.

Table 2: Coordinate Results for the CM and CB

Specification	x	y	z
Center of Mass	-0.008 in	-1.377 in	0.753 in
Center of Buoyancy	-0.001 in	-0.288 in	0.790 in

Because the center of mass is directly below the center of buoyancy, the AUV will be statically stable in rotation.

However, since the buoyancy is over 20lbs higher than the weight, it will not be statically stable in the 'up-down' direction.

Realizing that the need to counteract the vehicle's natural buoyancy and achieve a state of neutrality would require a significant amount of dead weight, the platform was redesigned to accommodate more elements [4].

Aluminum 6061 was tested for the AUV leg support and loaded with 60lbf, accounting for any extra weight beyond the estimated 50lbs necessary for the AUV to counteract buoyancy. The load for one leg is exaggerated, even though the load is shared between two, to observe the effects of stress based on material and geometry. The test confirms that under a severe weight bearing, the legs possess the capability to withstand great stress tolerances beyond the estimated total weight of the AUV. The stresses in the analysis falls below the maximum yield point, which is 40 kpsi. The deflection analysis also indicated that even at the point of maximum deflection, the stress is far from the maximum yield point. Even though the legs were manufactured, by first heating the metal with a blow torch and then manually bending the piece in a bending machine at pre-measured points, the respective analyses displayed in Fig. 18 and 19, held true.

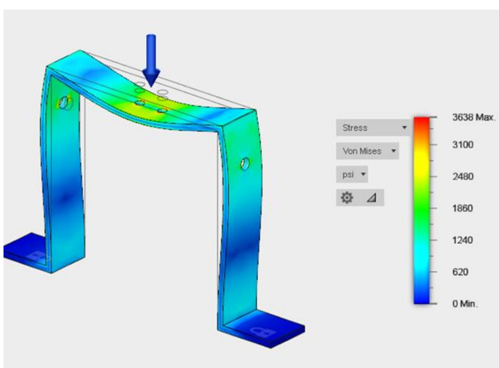

Fig. 18 Autodesk Fusion Rendering of CM and CB Coordinate Results

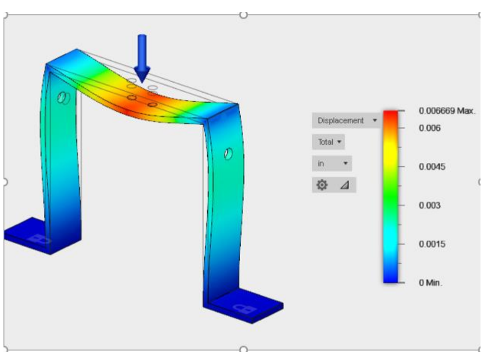

Fig. 19 Autodesk Fusion Rendering of CM and CB Coordinate Results

7) Mounting Brackets

The mounting brackets serve as a medium to attach the thrusters to the AUV. Each bracket is tailored to fit any thruster and can be moved in relatively any direction or relocated anywhere on the sub. There are two main types of brackets, the flat thruster plates (Fig. 20), which are designed to accommodate the side thrusters and the modified L-shaped mounting brackets (Fig. 21), which are designed to accommodate the four thrusters attached to the aluminum platform. The L-shaped brackets is made out of 3D printed ABS filament, due to the variances of the aluminum brackets in bending angles

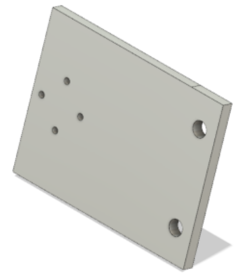

Fig. 20 Autodesk Fusion Rendering Flat of Thruster Plates

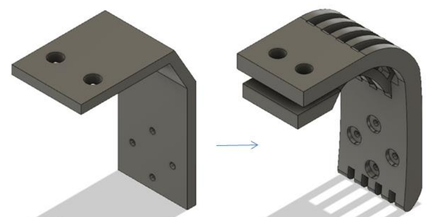

Fig. 21 Autodesk Fusion Rendering comparison of old to new updated L-brackets for Thrusters

C. Electrical Systems

The greatest lesson the team learned in the development and integration of the electrical system was contingency. Given the experiences of the teams in previous years, navigation and system control has continually been a problem for the PV AUV team. The second system was designed to complete the basic functionalities needed to carry out the aforementioned, navigational tasks, leaving room for expansion building towards the competition and future endeavors.

1) Power System

The *PV Inspire* can be powered by a single 14.8V, 20Ah or 16aH Li-Po battery, located on the second tray of the electronics control system rack (ECSR). The battery's capacity is sufficient to provide run time of at most 2 hours based on testing and observation from last year testing and trial runs.of which far exceeds the fifteen-minute time limits for actual and practice run segments of the competition.

The power supplied by the battery is conditioned by way of two solid-state relays (SSR), when individually switch enabled, distributes power through 2 branches within the electronic control system rack (ECSR). Switch one sources power through SSR-1, through to a LM2596 Buck Step-down DC voltage regulator which conditions the voltage to the recommended input operating parameters for the microcontroller boards. Switch two sources power through SSR-2, directly to a twelve-gang terminal block (TB-1), wired to individually power each of the electronic speed controllers (ESC) that operate its associated connected thruster. Uniquely assigned (addressed) output pins on the Arduino microcontroller is wire to each ESC, providing enabling control signals to the thrusters. The camera(s) are operated and controlled from a mini STX motherboard.

2) Computer and processing

Each functional component of *the PV Inspire* is operated by two primary processing components: the Arduino Mega 2560 and Intel Celeron. The Arduino is responsible for utilizing the Inertia Measuring Unit (IMU) in order to adjust the thrust based on orientation of the vehicle. The motherboard is for graphics processing of the camera for Originally, each board was responsible for one major component or functionality of the *Inspire*. However, based on limited time and complexity of the programming, most functionalities will be run using the Arduino Mega 2560. This will not include the camera which is working with the Intel Celeron.

IV. Experimental Results

Primary testing was directed to thoroughly waterproofing the hull as the aforementioned problems with the acrylic endcaps made this task impossible. After the remake of the endcaps and a change in lubrication, petroleum jelly to silicon grease, waterproofing was no longer an issue and allowed for the integration and implementation of the electronics. Plasti-dip was also used at the front of the hull to seal any small leaks the inevitably presented itself.

During this phase of testing, the team observed and confirmed that while the AUV maintained balance and was statically and dynamically stable, and by adding several removable dead weights presented a problem. Adding large preset that become a part of the main structure permanently where less removable weights were needed. Currently, certain components of the vehicle are being modified to help reduce buoyancy and add weight.

For the camera system, the lighting was added in order to improve color recognition underwater, but at the cost of larger voltage draw from the main electrical system. Coding was eventually added to reduce brightness or control the brightness based on the task pursued.

Although the thruster configuration has been completed, the programming for the camera processing, as well as the IMU and depth sensor is still being calibrated. Additional functionalities of the *PV Inspire* will be incorporated based on time. In the future, testing of the electronic components should begin during the first semester to minimize unforeseeable mishaps such defective or unnecessary parts. Extra consideration to minor details as well as improved accountability from individual teams, mechanical, electrical and computer engineering, will allow the collaborative team to arrange more testing time and less contingency options.

V. Acknowledgements

The Autonomous Underwater Vehicle Senior Design Team (PV AUV) would like to thank Naval Sea Systems Command (NAVSEA) for their continued technical support and sponsorship.

We would also like to acknowledge Dr. Xiaobo Peng and Dr. Paul O. Biney for continuing to support the project and team members.

[1] Moore, Steven W., Harry Bohm, and Vickie Jensen. Underwater Robotics: Science, Design & Fabrication. Monterey, CA: Marine Advanced Technology Education Center, 2010. Ch. 4. pp.157-202

[2] Moore, Steven W., Harry Bohm, and Vickie Jensen. Underwater Robotics: Science, Design & Fabrication. Monterey, CA: Marine Advanced Technology Education Center, 2010. Ch.5. pp. 203-205

[3] "Design Guideline for Radial Seals." *Engineering Fundamentals.* EFunda Inc., 2017. Web. 02 July 2017.

[4] Moore, Steven W., Harry Bohm, and Vickie Jensen. Underwater Robotics: Science, Design & Fabrication. Monterey, CA: Marine Advanced Technology Education Center, 2010. Ch. 6. pp. 247-250